Available online at www.sciencedirect.com

ScienceDirect

journal homepage: http://www.elsevier.com/locate/acme

Original Research Article

Potentials of in situ monitoring of aluminum alloy forging by acoustic emission

Bernd-Arno Behrens, Anas Bouguecha, Christian Buse, Kai Wölki, Adrian Santangelo *

Leibniz Universität Hannover, Institute of Forming Technology and Machines (IFUM), An der Universität 2, D-30823 Garbsen, Germany

ARTICLE INFO

Article history:
Received 19 February 2016
Accepted 23 April 2016
Available online

Keywords:
Forging
Process monitoring
Acoustic emission testing
Aluminum alloy

ABSTRACT

Deviations during forging processes lead to workpiece failure when the forming limits of the material are exceeded. In production processes an early detection of manufacturing faults is preferred. The acoustic emission (AE) technique is examined with respect to its ability to detect deviations in lubrication conditions and in the structural integrity of different aluminum part geometries and alloys during forming. In a first step, an upsetting of varying specimen shapes was performed in order to study correlations of occurring defects as well as changing friction conditions with acoustic emission response. Afterwards, a cross joint was forged and AE was analyzed. The results suggest that crack detection during forging is feasible but limited by material ductility. In addition, it is shown that the characteristics of the acoustic emission during forming strongly depend on the respective alloy. With respect to faultless warm forging it is found that different stages are reflected in the AE signal, facilitating the detection of process deviations.

1. Introduction

1.1. *Forging of Al-alloys*

Forged components are characterized by high mechanical strength under static as well as dynamic loads. These properties can be attributed mainly to a process-related reduced grain size, the well-distributed microstructure and their structural integrity compared to cast parts. With respect to energy and environment considerations lightweight material alloys are continuously gaining importance. Most processed metallic construction materials for lightweight applications are based on aluminum and there is an increasing trend of substituting bulk formed steel products with non-ferrous metal parts [1]. Aluminum alloys are characterized by a low density accompanied by a high mechanical strength compared to Fe-based alloys. Cold [2], warm [3] and hot forging [4] are possible with their respective advantages and disadvantages. In order to reduce long production times due to heat treatment and enhance shape accuracy, lower practicable forging temperatures are preferred in some cases. Here, the formability is reduced and the workpiece can react sensitively to changing process conditions resulting in a higher cracking risk. Generally, an early detection of failures is aimed at in production. In fast and automated forging processes cracks cannot always be recognized immediately.

* *Corresponding author*. Tel.: +49 511 762 2428; fax: +49 511 762 3007.
E-mail address: santangelo@ifum.uni-hannover.de (A. Santangelo).
http://dx.doi.org/10.1016/j.acme.2016.04.012

Another important aspect with regard to forging quality is friction. Adequate lubrication conditions between die and part play a crucial role with respect to the tool life and quality of finished parts. Insufficient lubrication can lead to excessive tool wear and improper strain distribution which in turn can result in defective parts or insufficient die filling.

Most commonly, the regularity of the forging process is inferred on-line from the force and displacement measurement of the ram. Nevertheless, process deviations are not always reflected by these signals.

A known non-destructive technique which has the potential to overcome the shortcomings of conventional measuring methods is the acoustic emission technique. Its capability to detect cracking in metallic materials and changes in the friction conditions between metals has been proven before [5,6].

1.2. *General aspects of acoustic emission technique*

The acoustic emission (AE) technique is a non-destructive evaluation technique enabling the user to draw conclusions in situ about the structural integrity of an object. Commonly, AE is defined as elastic waves which develop during the spontaneous release of energy in a solid body. According to this definition, it is an integral and passive inspection method with which an event can be detected during its occurrence, and only then. In view of their frequency range (50 kHz to several MHz), AE signals are considered as ultrasonic waves. In a typical measurement system these waves are received from solid body surfaces and are converted into a voltage signal by highly sensitive piezoelectric sensors. This signal passes a preamplifier, a frequency filter and an analog digital converter in order to finally be recorded by a storage medium. Much effort has already been put into understanding the mechanisms of acoustic emissions of static structures, but also into those of light metal alloys under plastic deformation [7,8]. Deformation, or more precise, dislocation glide is a strong source of acoustic emission. A further origin of AE is crack growth. Intensity and characteristics of the emitted waves depend on numerous material and testing variables including strain rate, forming temperature, grain size, solute content and stress state. The detection of crack growth is related to the ductility of a material. While one alloy can emit AE with high energy during cracking, other materials remain quiet which has been termed the ductile-crack problem [9]. The AE amplitude is connected to the velocity at which a crack propagates. That implies that sudden, fast propagating cracks will produce higher amplitudes than a slowly advancing crack tip over the same distance [10]. Moreover, the type of crack plays an important role: the tensile type is generally connected with a faster arrival time of peak amplitudes than the shear type [11].

The ability of monitoring friction conditions by means of AE was shown for different material combinations in tribometer test rigs [12,13]. Commonly, these studies are performed under stationary test conditions and in absence of macroscopic plastic deformation.

The property of an AE measuring system to detect structural changes at their moment of occurrence makes it a promising potential tool for the detection of process deviations during metal forming operations [14,15].

1.3. *Acoustic emission in aluminum forging*

Most research concerning AE during forming is done under idealized and highly controlled test conditions for comprehensible reasons. By using standardized and simply shaped specimens, conclusions can be drawn easily and reliably. Since the user is often confronted with unstable and more complex operation conditions, the research outcomes cannot always be transferred to industrial cases. Great part of this research work is focused on the characterization of AE in dependence of deformation parameters and the material state of Al-alloys. The detection of process deviations in industrial forging processes is often not the point of concern. The principal applicability for the determination of defects within light alloy forging parts during forming processes has been proven before, also under idealized conditions but closer to conventional forging in respect of forming speed and temperature [16]. It was also used to determine the limit criterion due to crack initiation in upsetting under superimposed pressure [17]. Despite all efforts undertaken so far, the AE technique is still not sophisticated enough for industrial forging applications. The challenge in establishing a reliable use of the AE technique in forging processes lies in their highly dynamic and transient character in contrast to static structures with a constant basic level of AE. Moreover, the harsh conditions in a forging environment and the multiple AE of tool and machine can complicate the analysis considerably. Another question is the general ability to detect the cracking of a certain alloy. The amount of AE energy emitted depends on material and deformation and is not known ex ante.

In another study it was found that a correlation between AE and lubrication condition in hot forging of aluminum exists [18]. It remains unanswered if such a correlation holds true for other forging processes. On the one hand high energy emission due to deformation could overlay friction signals, on the other hand surface condition and speed of the relative movement play a role.

The aim of this study is to investigate AE with regard to process deviations, namely cracking and lubrication, in the forging of different aluminum alloys from a practical point of view. For this purpose, upsetting and forging experiments were carried out and the recorded signals were correlated to the process deviations.

2. Material and methods

2.1. *Experimental setup*

For the experimental work, cylindrical specimens of the Al-alloys AW 5083, some strain-hardened (H112), AW 6082, AW 7075, solution heat-treated and artificially aged (T6/T6511) were used. The alloy 5083 was essentially recrystallized with peripheral coarse grains. The other two alloys showed a fibrous grain structure in extrusion direction, cf. Fig. 1.

The temperature of the specimens at the start of deformation ranged between room temperature and 450 °C. A hydraulic press with a maximum force of 12500 kN was used. The ram velocity was set to 1 mm/s and 28 mm/s. Additionally, a screw press with a gross energy of 15 kJ, a nominal force of 2500 kN and

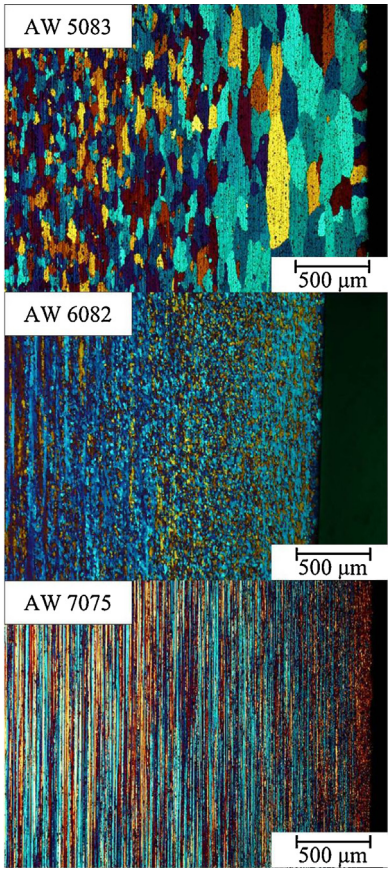

Fig. 1 – Metallography pictures of the near-surface zone of the billets.

an initial ram velocity of up to 300 mm/s was used for warm and hot forging with the same tool and equal AE acquisition setup. AE sensors were mounted directly on the die adapters by magnetic holders with a hold-down force of 50 N. One additional sensor was placed on the ram to identify AE that is not directly caused by the forming process (guard sensor). Signal acquisition was carried out with the AE measuring system AMSY-6, Vallen. Two types of sensors were attached to the tooling. A resonant sensor with a frequency range of 100–900 kHz (S2) and a peak frequency of about 350 kHz as well as a broadband sensor with a range of 200–2500 kHz (S1) were used. Filters were set to 95–850 and 520–1600 kHz respectively. A S1-identical sensor S3 was mounted on the base part and a S2-identical sensor S4 was placed on the ram. Fig. 2 shows a photo of the experimental test setup.

The voltage signal was amplified with 34 dB. The acquisition mode was continuous with a sampling rate of 5 MHz and 4096 samples per data set, so that the entire signal waveform as well as extracted signal parameters were recorded for defined time intervals. In addition, ram displacement was measured with an incremental draw wire sensor, force was measured with a strain gauge based load cell. The voltage output of the force and displacement devices was digitized and stored synchronously to the AE data with a sampling rate of 20 kHz. The tool system is modular. Depending on the forming process, both the upper and the lower die can be changed.

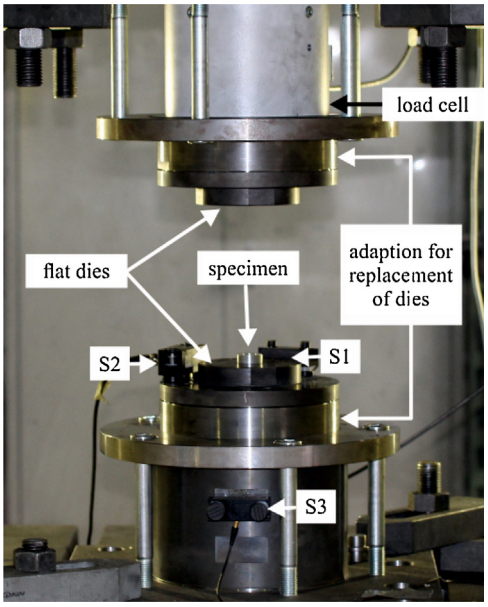

Fig. 2 – Model of forming tool system and experimental test setup for upsetting.

2.2. *Ring compression test*

In order to test the influence of lubrication on AE, ring compression tests were performed. The ring compression test is a frequently used method to determine friction factors between surfaces during plastic deformation in bulk metal forming processes [19]. Here, a ring with a commonly used ratio of 6:3:2 of outer to inner diameter to height is upset axially between two flat dies. Depending on the friction, the inner and outer diameter ratio results in different values after deformation. Under high friction, the inner diameter becomes small and increases with decreasing friction as drafted in Fig. 3.

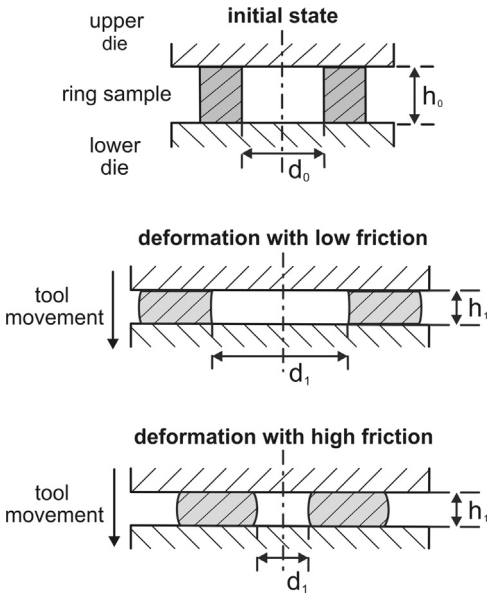

Fig. 3 – Principle of the ring compression test (section view).

The friction factor is determined from an analytically or numerically developed graph indicating the respective friction factor for each inner diameter. The combination of compressive deformation and high surface-to-volume ratio of the specimen renders this test ideal for analyzing lubrication conditions in conjunction with AE. For the ring compression tests the alloy 6082 was chosen due to its low overall AE amplitude level during deformation. Deformation-related AE would be regarded as noise in this case. The height reduction was 60% and the ram velocity was set to 1 mm/s both, in dry condition and with the use of a mineral-oil-based lubricant. Die surfaces were polished prior to the tests.

2.3. *Upsetting test*

Upsetting experiments were conducted with two different specimen geometries and five upsetting tests per geometry and alloy. Cylindrical specimens with a diameter of 25 mm and a height of 36 mm as well as specimens with collar were upset, see Fig. 4, in order to relate deformation and cracking to resulting AE characteristics in a simplified bulk forming operation.

With the upsetting of the cylinders a conclusion about the strain-dependent AE can be drawn and differences in AE activity until fracture can be observed. By upsetting until cracking, the resulting AE signal amplitudes can be used as an indication for the signal intensity of each alloy. The two different specimen geometries exhibit different modes of cracking. The specimen type with collar enables locally defined cracking due to tensile stress concentrations at the collar, i.e. opening mode. Cylinder failure manifests itself in shear cracking, i.e. sliding mode. The specimens were upset to final heights from 25 to 9 mm, depending on the starting point of cracking. They were upset without lubrication and at room temperature. Additionally, for the purpose of increasing ductility, three specimens with collar of each alloy were heated up to 150 °C and deformed with a time lag of up to 5 s.

2.4. *Forging of a cross joint*

Demonstrative parts with the geometry of a cross joint with flash were forged. For this, the flat dies were replaced by molded dies on the same tool system. Thus, forging conditions remained the same and comparability with the foregoing upsetting test is given. The billets had a diameter of 25 mm and heights of 28 and 36 mm. Heating of the dies was waived due to the limitation of the sensors used to temperatures below 100 °C. Moreover, the probability of cracking is increased without heating. The cavity is constructed in a way that the contact zones, the areas with the highest heat loss, coincidentally are dead zones with minimum deformation. A series per alloy was formed to three intermediate stages of 2, 4 and 6 mm before the final height of the forged cross joint. By examining the part surface in the intermediate stages, the time interval for the onset of cracking can be determined.

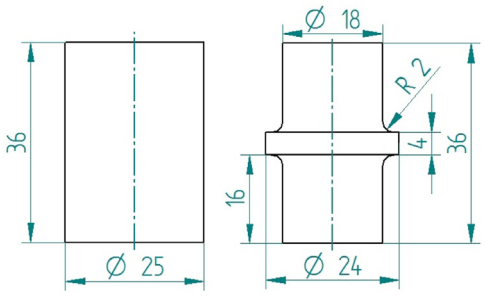

Fig. 4 – Dimension of specimens for upsetting.

3. Experimental results and discussion

3.1. *Testing of the measuring setup*

Before the execution of the experiments, the measuring setup (press and tooling system) was tested for noise and quality of sound transmission. For this purpose, a cylindrical specimen was placed between the dies and loaded with the ram weight of 8 tons. A pencil lead of 0.5 mm diameter was broken several times in a defined angle known as Hsu–Nielsen source directly on the surface of the specimen and occurring signals were recorded. The maximum signal amplitude for a time interval of 819.2 μs is represented by one dot in the graph in Fig. 5.

Despite the boundary between specimen and die, there is an excellent sound transmission with the resonant sensor S2 followed by the broadband sensor S1. The effect of an additional barrier becomes obvious with the S1-identical sensor S3 that was mounted on the base part and a S2-identical sensor S4 that was placed on the ram. Due to their good positioning only the sensors S1 and S2 were considered for signal analysis.

In addition, machine noise was tested while moving the ram with varying velocities without load. In case of S1, there was no effect on the signal identified. The background noise of S2, however, correlated positively with the ram velocity for 28 mm/s with about 38 dB, for 10 mm/s with about 32 dB and for 1 mm/s with 26 dB. A detailed analysis of the frequency spectrum by a fast Fourier transform (FFT) revealed that the peak frequency range of machine noise was up to 150 kHz. That is the reason why S1, whose lower limit of the bandpass was set to 520 kHz, is insensitive.

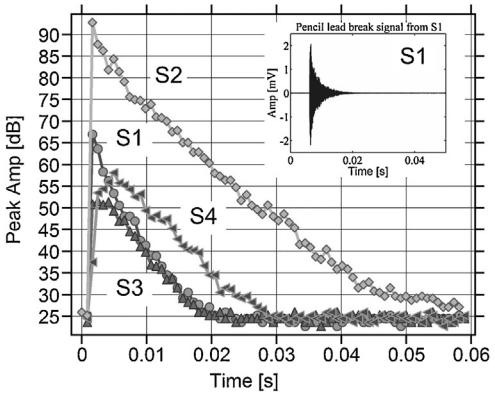

Fig. 5 – Amplitude/time correlation for pencil lead break for different AE sensors and sensor positions.

3.2. *Ring compression test*

The correspondent friction factors in the ring compression tests were calculated as 0.35 with lubrication and 0.65 under dry conditions. A visual examination of the surface showed differences in roughness. In contrast to dry friction which resulted in smooth surfaces, the lubricant caused a coarse surface with concentric small cracks due the low formability of the aged alloy. Despite the considerable differences in friction and surface quality there was only little effect on the acoustic emission in terms of signal amplitudes. Only deformation with a ram velocity of 1 mm/s is considered, since in this case machine noise is on a low level. While sensor S1 transduced nearly no activity, voltage from S2 was low but increased during compression. The graph in Fig. 6 shows the mean of the root mean square (rms) of five arithmetically averaged signals per friction condition.

The curves are enveloped by their standard deviation. The rms is built for intervals of 607200 data points that equals a time interval of 0.12144 s. It can be stated that for the given surfaces and dimensions a change in lubrication condition is reflected only to a poor extent in the calculated rms. The envelopes of standard deviation overlap partially. Forming processes with high AE activity due to deformation would not allow an assessment of friction conditions in the investigated dimensional scale.

3.3. *Upsetting of cylindrical specimens*

The upsetting tests at room temperature revealed the very good ability to detect cracking during deformation for all three types of alloy. A dependence of AE on the chemical composition during forming can be stated. In Fig. 7 exemplary results of upsetting for the three alloys at a ram velocity of 28 mm/s and 1 mm/s are depicted as an amplitude/displacement correlation.

To prevent a severe fracture of the alloy 7075 due to its low ductility a ram velocity of 1 mm/s was chosen. Each point represents the amplitude of a time window of 819.2 μs

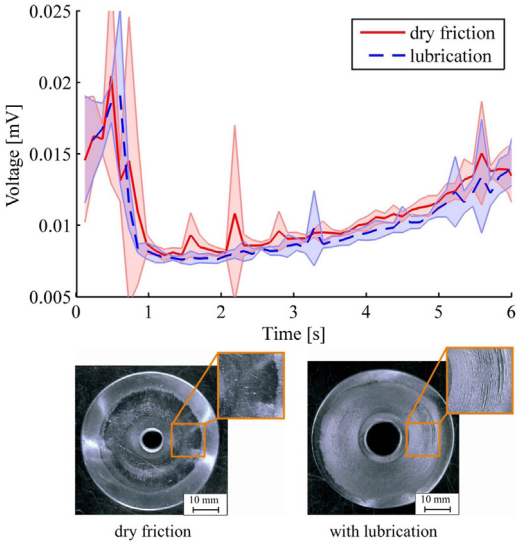

Fig. 6 – Root mean square and standard deviation as envelope for ring compression test.

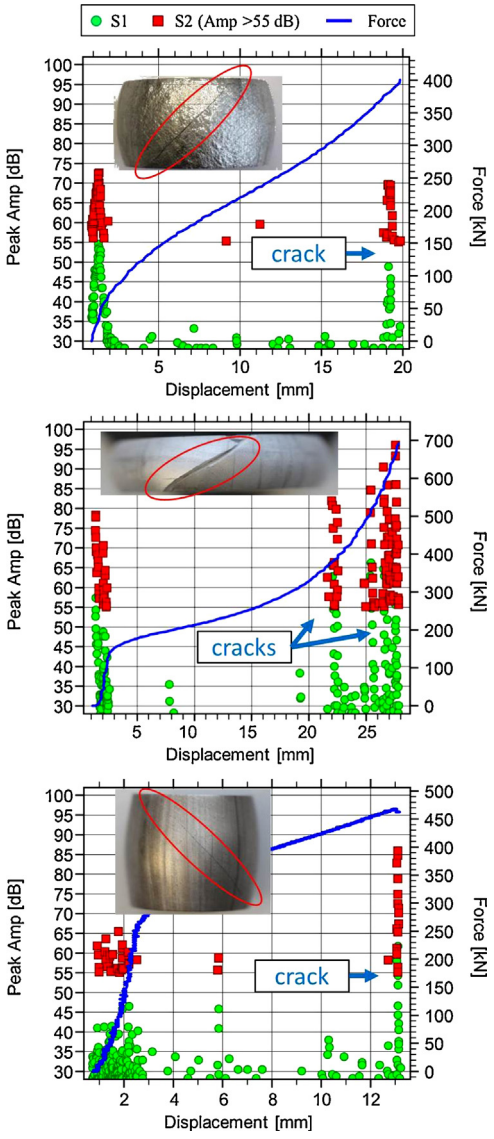

Fig. 7 – Amplitude/displacement correlation of two different AE sensors for Al-alloys AW 5083 (top), 6082 (center) at ram velocity 28 mm/s and 7075 (bottom) at ram velocity 1 mm/s during upsetting.

recorded by sensors S1 and S2. For a better visual clarity, amplitudes of S2 were cut at 55 dB. In all cases the transition from elastic to plastic deformation is connected with high-energy AE that attenuates during plastic deformation. The moment of failure is marked by a short and sudden increase in amplitude. 6082 was damaged severely on different locations due to excessive reduction and shows high AE amplitudes over a wider range of deformation. The resulting 45 ° shear cracks are indicated by an oval on the photos in Fig. 7. The 5083 specimens showed a remarkably rough surface due to coarse grains at the boundary zone.

3.4. *Upsetting of specimen with collar*

In contrast to the shear-type cracks of the cylindrical specimens, the cracks of the specimens with collar were longitudinal. These

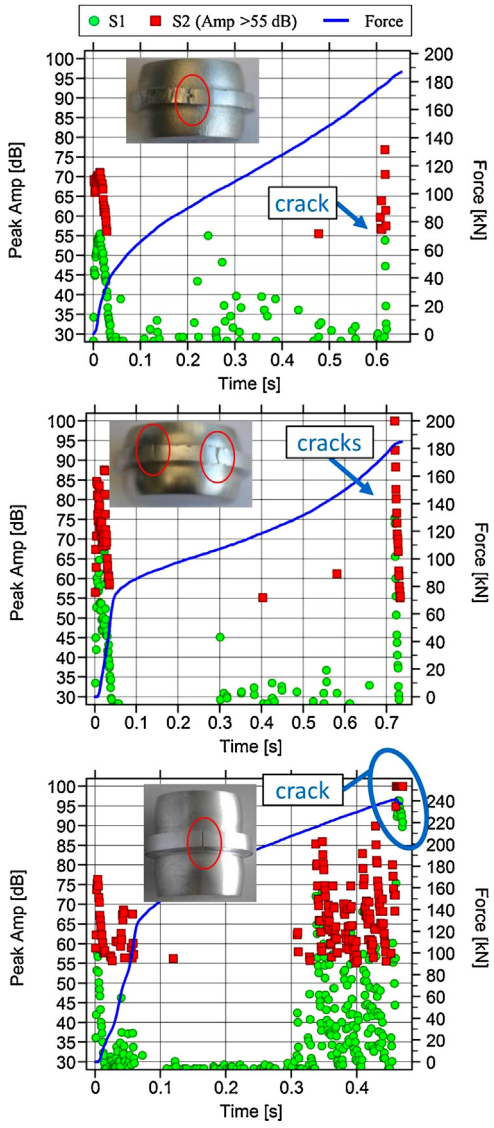

Fig. 8 – Amplitude/time correlation of two different AE sensors for Al-alloys AW 5083 (top), 6082 (center) and 7075 (bottom) during upsetting of specimens with collar at room temperature.

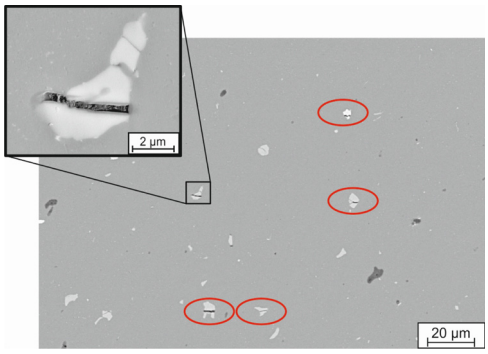

Fig. 9 – Metallography picture from the collar region of deformed Al-alloy AW 7075 containing fractured intermetallic particles.

cracks were also connected with high AE amplitudes for cold forming. Exemplary results for the alloys 5083, 6082 and 7075 are shown in Fig. 8.

The high amplitudes toward the end of stroke indicate cracking and are marked by an oval. 5083 was reduced to 18.5 mm, 6082 to 16.5 mm and 7075 to 25 mm. On 6082 samples crack detection was irregular and crack indicating amplitudes were not always existent. Upon comparing the graphs, different AE intensities along the deformation path become obvious. As in the upsetting of the cylinders, cracking is also indicated by high signal amplitudes, characterized by a sudden increase and short duration. With 7075 strong AE activity started reproducibly after 8 mm stroke (=Ã0.3 s) and remained until the end of stroke. This phenomenon was not observed with the other alloys. Metallographic analyses of specimens after deformation suggest that this strong activity might be caused by the fracture of intermetallic particles, cf. Fig. 9.

Findings on tensile tests that describe a strong correlation between AE counts[1] and number of cracked particles support this conjecture [20]. This observation can be useful to detect an early stage of damage on a microstructural scale. Further experiments on 7075 were performed with annealed specimens. The described high-amplitude emissions directly before the cracking event were absent. Cracks were also detected reliably in this case, although the amplitude was reduced.

An important conclusion as to the nature of crack initiation and propagation can be made by analyzing the duration of the crack burst. After the occurrence of the crack in the collar its stable propagation into the sample is not further connected with changes in the AE signal.

In equal experiments on specimens at 150 °C, cracks could be identified unambiguously by the AE amplitude in the case of 5083 and 7075. 6082 instead remained nearly completely without an AE response. Upon comparing the signals in Fig. 10, the differences become obvious. Due to the enhanced formability of the alloys in contrast to cold forming 6082 was reduced to a height of about 9 mm and 7075 to 14 mm.

While 7075 shows a strong energy release due to material failure in 6082 high amplitudes are reached only by a few short bursts. These are not likely connected with the material failure due to their very short duration. Having a closer look at the crack quality of the 7075, the corresponding waveform reflects the cracking of the collar and its transition to the main body by two main bursts. At 300 °C no cracks could be identified in 5083 by AE evaluation. At this temperature, the ductility of 7075 had increased so much that cracking on the collar could not be achieved for the used reduction ratios.

Besides cracking-induced AE, additional deformation-related AE were observed and are worth mentioning, since they might influence failure detection. Analyzing the AE in a lower frequency range recorded via sensor S2 while upsetting 5083, a signal pattern can be recognized known as Portevin–Le Châtelier (PLC) effect. The PLC effect is an unstable plastic flow that manifests itself in serrated stress–strain curves in

[1] Counts are the number of crossings of a defined threshold voltage.

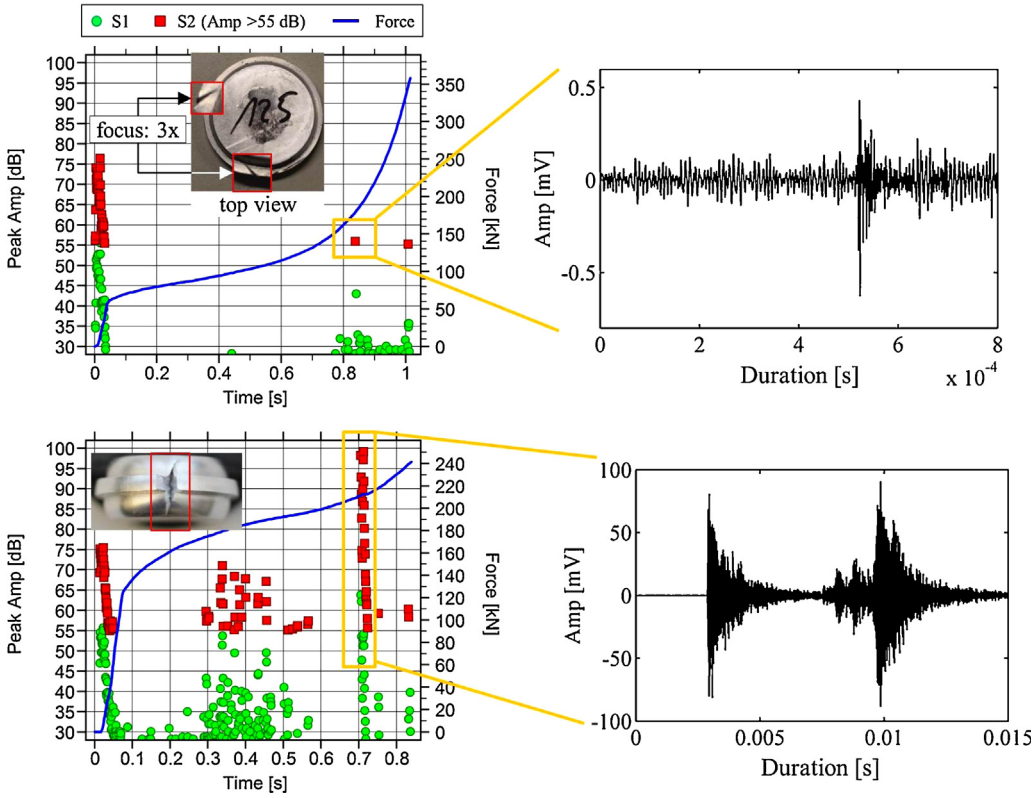

Fig. 10 – Comparison of amplitude/time correlation for Al-alloys AW 6082 (top) and 7075 (bottom) during upsetting of specimens with collar at 150 °C.

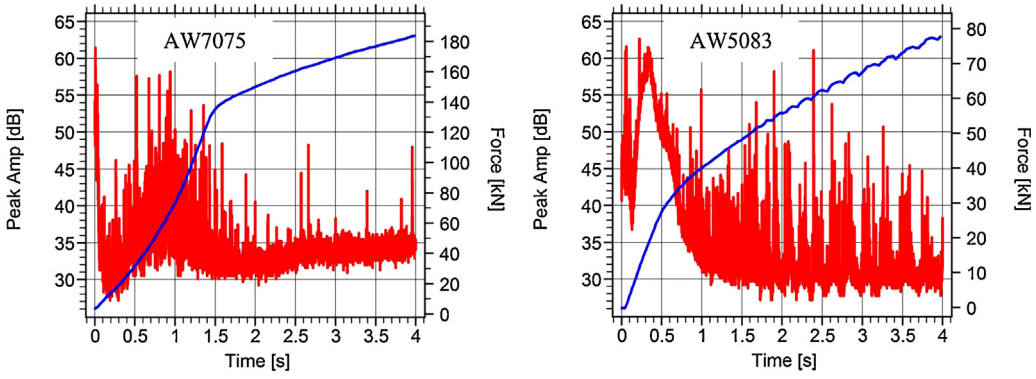

Fig. 11 – Amplitude/time correlation from AE sensor S2 for Al-alloys AW 7075 (left side) and 5083 (right side) during upsetting of specimens with collar at 1 mm/s.

some Al-alloys, among others under certain deformation conditions [21]. The dependency of AE-bursts on stress drops is known and was rather investigated on tensile tests [22]. In Fig. 11 the amplitude/time correlations for the first 4 mm of the stroke at a ram velocity of 1 mm/s for 7075 (left side) and 5083 (right side) are compared.

The graph for the upsetting of 5083 clearly shows the jumps in amplitude caused by the PLC effect. Its occurrence can be confirmed by the serrated force–time curve. Additionally, with respect to deformation-related AE, it is apparent that the transition from elastic to plastic deformation has a much broader amplitude spectrum for 7075.

3.5. *Forging of a cross joint*

The forging of the three alloys at room temperature caused cracking in all cases which were related with significant AE signals. By forming the part to intermediate stages, the onset of cracking could be determined visually. Fig. 12 contains a photo of parts from different cold forming stages.

In Fig. 13 the amplitude/time correlation for an intermediate forging stage at 4 mm before the end of stroke of a cross joint made of 5083 is depicted.

Three cracks were visible in the flash zone of the part. Defects occur after the material has entered the forming elements of the

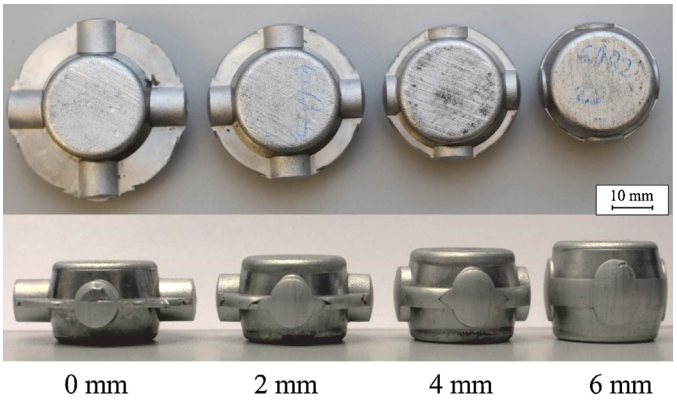

Fig. 12 – Intermediate forming stages of a cross joint made of AW 6082.

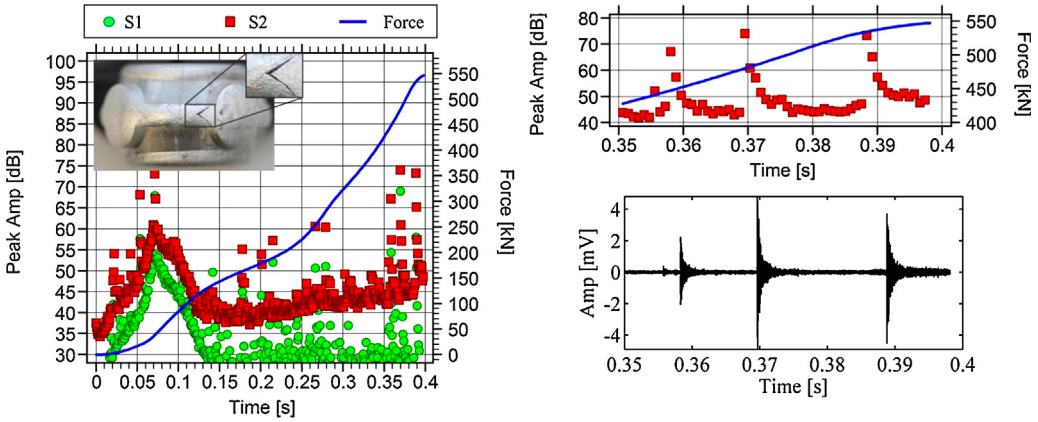

Fig. 13 – Amplitude/time correlation of two different AE sensors during cold forging of a cross joint made of AW 5083.

cross, i. e. just before the stroke of the depicted part has ended. Crack-related AE are identified by point in time, intensity and burst character. During forging at 150 °C, the deductibility of cracks from the AE signal became very poor as amplitudes were low or even vanished completely. This is attributed to the small crack size and enhanced ductility at higher temperatures. Especially in the case of 6082 no significant emissions were recorded at the assumed forming interval for cracking. In addition to the low energy of crack-related AE at a higher ductility state of the material a reliable distinction is considerably hampered by overlaying deformation-related AE. Due to multiple possible sources of AE during the forging process the differentiation of relevant signals from irrelevant ones is an important task. Therefore, a classification of the signals that go beyond the amplitude is required. This is made by comparing signal features of individual bursts, as shown exemplary in Fig. 14.

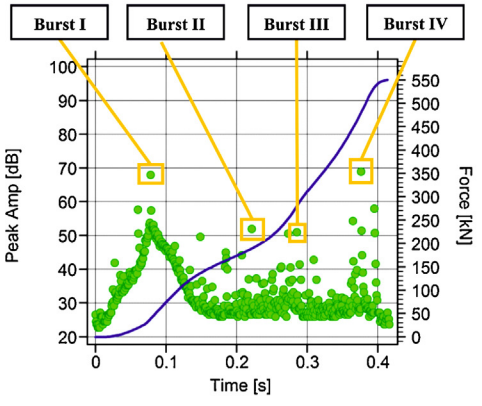

Features	Burst I	Burst II	Burst III	Burst IV
Risetime/Amplitude [ms/V]	305800	18200	2300	361
Average-Frequency [kHz]	502	135	198	562
Counts	507	10	71	561
Partial Power Band 500-750 kHz [%]	18.72	26.04	32.13	56.10
Partial Power Band 750-1000 kHz [%]	24.55	26.06	23.73	23.20
Duration [µs]	819	819	819	819
Frequency Center of Gravity [kHz]	1035	917	859	937
Frequency of Max. Amplitude [kHz]	722	902	714	691

Fig. 14 – Evaluation of different features of selected bursts from cold forging of a cross joint.

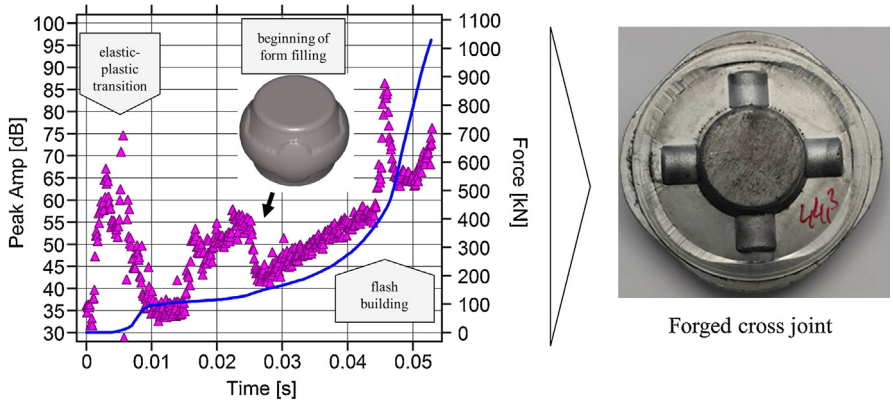

Fig. 15 – Amplitude/time correlation of AE sensor S2 during forging of a cross joint made of AW 6082 at 300 °C on a mechanical press.

A threshold crossing of 0.1 mV and a duration of 819 μs were set as burst definition. Only burst IV is connected with a macroscopic cracking. Some of the feature values correlate with the signal's energy content. The entire feature vector can allow a classification and differentiation. This is especially useful for signal windows with equal maximum amplitudes. The major drawback for the establishment of a classification algorithm is that an extensive training data set has to be acquired.

Beyond cracks it was observed in defect-free warm forging that some stages of the forming path are reflected in the AE amplitude. These stages became more evident when forging was performed on a mechanical press with high ram velocity. Fig. 15 shows the amplitude/time correlation for the entire forming path of a billet of 6082 with an initial height of 36 mm and temperature of 300 °C, resulting in excessive flash.

The dots represent the maximum signal amplitudes for a time interval of 102.4 μs. Three regions are characterized when the course of the AE signal is analyzed and related to the forming stages. The process starts with an upsetting visible in the typical hill-shaped AE amplitudes at the transition from elastic to plastic deformation followed by the guided lateral flow where form elements begin to get filled. This stage is connected with a second amplitude hill. The final characteristic region is marked by an amplitude jump. At this point, the form is completely filled and only flash is built. This relation is suitable for practical use as it could allow for an assessment of the process with respect to form filling.

4. Conclusion

In this work, the potential of the AE technique for the detection of manufacturing faults and deviations during forging was examined for three different aluminum alloys. With respect to friction, there was merely weak evidence that deviations can be detected with the help of AE on the used test rig and AE acquisition setup. However, studies in lower frequency ranges and other surface dimensions or conditions are worth being performed in the future as a higher AE energy release might be possible in other cases. Further, it can be noted that the examined materials can exhibit very different AE characteristics. The alloy 5083 is susceptible to a PLC effect causing high AE activity. A high AE intensity could also be caused by fracture of inclusions in case of 7075. While up to a billet temperature of 150 °C the high-strength material 7075 allowed for an excellent crack detection for opening cracks in collar specimens, this was possible on 6082 only at room temperature. It can be concluded from the forging experiments that the application of the acoustic emission technique on processes with form elements is principally feasible, but its success strongly depends on the used alloy, state and temperature. It can be stated that the lower the ductility the higher the crack-related AE energy. The performed studies suggest that cold forging has to be favored over warm or hot forging when the AE technique is considered for on-line crack detection. And even then it must be borne in mind that the ability of crack detection changes with the used material. A foregoing material characterization with simplified geometries is useful to examine this. As a main drawback for crack detection it should be mentioned that the guided flow of the material in real forging processes and the resulting local high strains and strain rates can impede the signal analysis due to overlaying deformation-related noise. Noise emitted by machines and environment is a further aspect to be considered. An evaluation of feature vectors can be a way to overcome such shortcomings. Finally, potential of identifying process deviations with respect to form filling in faultless warm forging operations was identified.

Acknowledgements

The presented work is a result of the project ‘‘Online-Überwachung von Schmiedeprozessen mittels akustischer Emissionsanalyse’’, project number BE1691/78-2, granted by the German Research Foundation (DFG) The authors are thankful for the financial support. Thanks to Institut für Werkstoffkunde (Materials Science), Leibniz Universität Hannover, for scanning electron microscope images.

REFERENCES

[1] B.-A. Behrens, R. Nickel, S. Müller, Flashless precision forging of a two-cylinder-crankshaft, Production Engineering 3 (4–5) (2009) 381–389. http://dx.doi.org/10.1007/s11740-009-0185-x.

[2] A. Forcellese, F. Gabrielli, Warm forging of aluminium alloys: a new approach for time compression of the forging sequence, International Journal of Machine Tools and Manufacture 40 (9) (2000) 1285–1297. http://dx.doi.org/10.1016/S0890-6955(99)00127-3.

[3] H. Yoshimura, Examples of precision forging by enclosed-die forging, in: 10th International Cold Forging Congress 2000, VDI Berichte, vol. 1555, VDI Verlag, Düsseldorf, 2000, pp. 151–161.

[4] M. Kleiner, M. Geiger, A. Klaus, Manufacturing of lightweight components by metal forming, CIRP Annals – Manufacturing Technology 52 (2) (2003) 521–542. http://dx.doi.org/10.1016/S0007-8506(07)60202-9.

[5] K. Ono, Current understanding of mechanisms of acoustic emission, The Journal of Strain Analysis for Engineering Design 40 (1) (2005) 1–15. http://dx.doi.org/10.1243/030932405X7674.

[6] V.A. Baranov, Acoustic Emission in Friction, Tribology and Interface Engineering Series, 53, Elsevier, Amsterdam, 2006.

[7] C.R. Heiple, S.H. Carpenter, Acoustic emission produced by deformation of metals and alloys. Pt. 1. A review, Journal of Acoustic Emission 6 (3) (1987) 177–204.

[8] C. Scruby, H. Wadley, J.E. Sinclair, The origin of acoustic emission during deformation of aluminium and an aluminium-magnesium alloy, Philosophical Magazine A 44 (2) (1981) 249–274. http://dx.doi.org/10.1080/01418618108239532.

[9] H.N. Wadley, C.B. Scruby, J.H. Speake, Acoustic emission for physical examination of metals, International Metals Reviews 25 (1) (1980) 41–64.

[10] C. Hellier, Acoustic emission testing, in: Handbook of Nondestructive Evaluation, McGraw-Hill, New York, 2001 (chapter 10).

[11] D.G. Aggelis, E.Z. Kordatos, T.E. Matikas, Monitoring of metal fatigue damage using acoustic emission and thermography, Journal of Acoustic Emission 29 (2011) 113–122.

[12] H.S. Benabdallah, D.A. Aguilar, Acoustic emission and its relationship with friction and wear for sliding contact, Tribology Transactions 51 (6) (2008) 738–747. http://dx.doi.org/10.1080/10402000802044324.

[13] C.L. Jiaa, D.A. Dornfeld, Experimental studies of sliding friction and wear via acoustic emission signal analysis, Wear 139 (2) (1990) 403–424.

[14] B.-A. Behrens, A. Santangelo, C. Buse, Acoustic emission technique for online monitoring during cold forging of steel components: a promising approach for online crack detection in metal forming processes, Production Engineering 7 (4) (2013) 423–432. http://dx.doi.org/10.1007/s11740-013-0452-8.

[15] B.-A. Behrens, I. El-Galy, T. Huinink, C. Buse, Online Monitoring of Deep Drawing Process by Application of Acoustic Emission, in: G. Hirt (Ed.), 10th International Conference on Technology of Plasticity, ICTP 2011, Steel research international Special edition, Verl. Stahleisen GmbH, Düsseldorf, (2011) 385–389.

[16] B.-A. Behrens, T. Hagen, J. Knigge, I. Elgaly, T. Hadifi, A. Bouguecha, New trends in forging technologies, AIP Conference Proceedings 1353 (1) (2011) 380–385. http://dx.doi.org/10.1063/1.3589545.

[17] B.-A. Behrens, T. Hagen, A. Klassen, J. Knigge, J. Mielke, I. Pfeiffer, Forging of aluminium components under a superimposed hydrostatic pressure to induce local strain hardening, Advanced Material Research 137 (2010) 191–217. http://dx.doi.org/10.4028/www.scientific.net/AMR.137.191.

[18] C.K. Mukhopadhyay, S. Venugopal, T. Jayakumar, S.L. Mannan, B. Raj, B. Chatterji, R. Srinivasan, V. Gopalakrishnan, G. Madhusudan, R.S. Tripathi, Acoustic emission (AE) monitoring of open die and closed die forging processes of Al alloy, Materials and Manufacturing Processes 22 (7) (2007) 887–892. http://dx.doi.org/10.1080/10426910701448974.

[19] K.P. Rao, K. Sivaram, A review of ring-compression testing and applicability of the calibration curves, Journal of Materials Processing Technology 37 (1) (1993) 295–318.

[20] M. Lugo, J.B. Jordon, M.F. Horstemeyer, M.A. Tschopp, J. Harris, A.M. Gokhale, Quantification of damage evolution in a 7075 aluminum alloy using an acoustic emission technique, Materials Science and Engineering A 528 (22–23) (2011) 6708–6714. http://dx.doi.org/10.1016/j.msea.2011.05.017.

[21] A. Yilmaz, The Portevin–Le Châtelier effect: a review of experimental findings, Science and Technology of Advanced Materials 12 (6) (2011) 63001 http://dx.doi.org/10.1088/1468-6996/12/6/063001.

[22] F. Chmelík, A. Ziegenbein, H. Neuhäuser, P. Lukáč, Investigating the Portevin–Le Châtelier effect by the acoustic emission and laser extensometry techniques, Materials Science and Engineering A 324 (1–2) (2002) 200–207. http://dx.doi.org/10.1016/S0921-5093(01)01312-0.